Electrical properties of epitaxial junctions between Nb:$SrTiO_3$ and optimally doped, underdoped, and Zn-doped $YBa_2Cu_3O_{7-\delta}$

W. Ramadan,[1] S. B. Ogale,[1] S. Dhar,[1] L. F. Fu,[2,3] S. R. Shinde,[1] Darshan C. Kundaliya,[1] M. S. R. Rao,[1] N. D. Browning,[2,3] and T. Venkatesan[1]

[1]*Center for Superconductivity Research, Department of Physics, University of Maryland, College Park, Maryland 20742-4111, USA*

[2]*Department of Chemical Engineering and Materials Science, University of California Davis, One Shields Ave., Davis, California 95616, USA*

[3]*The National Center for Electron Microscopy, Lawrence Berkeley National Laboratory, One Cyclotron Road, Berkeley, California 94720, USA*

(Received 7 April 2005; revised manuscript received 2 September 2005; published 22 November 2005)

Epitaxial thin films of optimally doped, underdoped, and Zn-doped $YBa_2Cu_3O_{7-\delta}$ (YBCO) were grown on single crystal (001) Nb:$SrTiO_3$ substrates by pulsed laser deposition (PLD) and the electrical properties of the corresponding interface junctions were examined. The growth conditions were optimized in each case to get the appropriate crystalline quality of the films as well as the desired normal state and superconducting properties. The films or heterointerfaces were characterized by x-ray diffraction, Rutherford backscattering (RBS) ion channeling spectrometry in normal and oxygen resonance modes, magnetic susceptibility, four probe in-plane resistivity, and the temperature dependent current-voltage (*I-V*) characteristics. Nonlinear *I-V* curves (forward and reverse) were obtained in all the cases, revealing some characteristic differences and interesting temperature evolution. These data, when analyzed within the framework of a standard description of transport across the metal-semiconductor (Schottky) interface, suggest lateral intrinsic nanoscale electrical inhomogeneity in the system. Also as compared to the case of optimally doped YBCO a small but definitive lowering of the effective Schottky barrier height Φ_B is observed for junctions based on oxygen underdoped and Zn-doped YBCO.

DOI: 10.1103/PhysRevB.72.205333 PACS number(s): 73.30.+y, 73.40.−c, 73.61.Ga, 74.78−w

I. INTRODUCTION

Interfaces between two dissimilar materials have always been a subject of great scientific curiosity and technological interest.[1–10] With the significant advances in thin film growth and characterization techniques over the past decade, the interest in the formation and properties of high quality, atomically flat and well characterized interfaces in epitaxial heterostructures has grown dramatically.[9–18] Indeed, such interfaces are now being looked at as new materials with unique properties,[13,15,16] capable of supporting novel device functions. Amongst the various interface systems, the semiconductor-semiconductor (*p-n* junction) and metal-semiconductor (Schottky) interfaces are perhaps the most widely studied in view of their widespread applicability in microelectronics technology. Not surprisingly, most theoretical considerations have also been directed to these interfaces and the same have matured over the years especially in the context of the electrical transport across interfaces.[19–27] However, with the ever shrinking dimensions of devices and the corresponding physics as well as processing problems faced by conventional semiconductor microelectronics,[28–30] attention is now being directed to new materials with high carrier concentration and the related interface systems. Towards this end, metal oxides such as the high temperature superconductors, colossal magnetoresistive managanites and transparent conducting oxides are being actively investigated.[31–36] The ongoing research on oxide-oxide and semiconductor-oxide interfaces is envisaged to lay the foundations of a potentially novel oxide electronics. Most efforts in this domain have been primarily directed towards the growth and microstructural characterization of epitaxial interfaces, and the measurements of the electrical properties of the interfaces are now beginning to grow.[37–47]

In this work we have examined the growth and properties (structural and electrical) of the interface between an oxide superconductor $YBa_2Cu_3O_{7-\delta}$ (YBCO) and an *n*-type oxide semiconductor 0.5 wt. % Nb-doped $SrTiO_3$ (NSTO). We have considered three different cases of optimally doped, oxygen underdoped and Zn-doped YBCO grown epitaxially on NSTO. The normal state and superconducting properties for all the three cases are known to be intriguing and continue to interest the scientific community for over a decade.[48–56] In addition to the basic characterizations of materials properties, we have focused on the temperature dependence of the *I-V* characteristics. We have analyzed the data in terms of the standard physical picture of a metal-semiconductor (Schottky) interface[20] and have extracted potentially useful information regarding the barrier properties.

II. EXPERIMENT

In our experiments commercially procured (Crystek) high quality single crystalline (001) 0.5 wt. % Nb-doped $SrTiO_3$ single crystal substrates were used for film growth. The YBCO films were grown by pulsed laser deposition (PLD) technique. A pulsed KrF Excimer laser was used for ablation. The corresponding energy density and pulse repetition rate were 1.8 J/cm^2 and 10 Hz, respectively. For optimally doped YBCO, the films were grown at 200 mTorr oxygen pressure

 ©2005 The American Physical Society

at the substrate temperature of 800 °C and then cooled to room temperature in oxygen pressure of 400 Torr. This growth condition is known to yield films with good crystallinity and superconducting properties.[57–59] Some films were also grown at 750 °C, to explore the effect of growth temperature on the electrical properties of the interface. One set of the optimally doped ($T_c \sim 91$ K) films were annealed at about 300 °C for several hours to achieve the desired degree of oxygen deficiency and underdoping. A separate set of Zn-doped YBCO films ($YBa_2Cu_{3-x}Zn_xO_{7-\delta}$, $x=0.2$) were grown at 750 °C at 130 mTorr oxygen and cooled under 400 Torr oxygen. This low temperature growth procedure was used to control the Zn loss at high temperature as suggested by Ogale *et al.*[60] The films were characterized by x-ray diffraction (structural quality, lattice parameter), Rutherford backscattering (RBS) channeling (crystalline quality, composition, thickness), oxygen resonance RBS technique (oxygen stoichiometry), and four probe electrical measurements. Indium contacts were made to NSTO while In-Ag contacts were made to the YBCO layer. This ensured ohmic contact characteristics. The approximate contact area in all cases was about 0.1 cm^2. The resistivity values for the superconductor films were measured on a pure $SrTiO_3$ (001) substrate, on which films were grown concurrently with those on NSTO, to avoid the interference of the conductivity of NSTO in the measurement. For the standard RBS and ion channeling measurement 2 MeV He ions were used. For the RBS oxygen resonance study the He ion energy was set to 3.05 MeV which enhanced the oxygen signal dramatically allowing oxygen detection in films with an accuracy of a few percent. We should like to point out that the data reported and analyzed in this paper were reproduced at least in three samples in each case.

III. RESULTS AND DISCUSSION

The details regarding the structural and compositional properties of films grown under the described conditions have been discussed previously. Specifically, the x-ray diffraction (XRD) patterns for all the three samples can be indexed to the (00ℓ) family of the 123 superconducting phase up to $\ell=11$ indicating their c-axis orientation. In Fig. 1 we summarize the results of RBS, ion channeling and oxygen determination studies. Figure 1(a) shows the representative RBS angular scan for the optimally doped sample. A good minimum channeling yield ($\chi_{\min}$) of 8% is realized, reflecting the high crystalline quality and epitaxial nature of the film. The minimum channeling ($\chi_{\min}$) yields for the oxygen deficient and Zn-doped films were 13% and 22%, respectively. The higher $\chi_{\min}$ values in these samples reflect defect-strain related local distortions of the matrix due to oxygen vacancies or Zn substitution, and are indeed expected to be revealed by the highly site distortion sensitive RBS ion Channeling technique.[53] We employed the oxygen resonance detection to explore the changes in the oxygen stoichiometry, both in the normal and channeling modes. From Fig. 1(b) (upper panel) it can be seen that the oxygen stoichiometry for the Zn-doped case is almost the same as that for the optimally doped sample. This is again consistent with the fact that Zn dopant substitutes for the Cu ions in the CuO_2 plane sites with the same valence state and thus the oxygen concentration is expected to remain undisturbed.[51,55] As shown in Fig. 1(c) (upper panel), the oxygen deficient sample has about 5% (±2%) less oxygen as compared to the optimally doped sample, when the integrated areas under the resonance peak are compared for the two cases. If we assume the oxygen stoichiometry ($7-\delta$ $YBa_2Cu_3O_{7-\delta}$) for the optimally doped sample to be about 6.93 ($\delta=0.07$) based on the observed transition temperature of 91 K, we obtain the $7-\delta$ value of about 6.6 ± 0.1 ($\delta=0.4$) for the oxygen deficient sample. As expected, this corroborates well[52] with the observed transition temperature of about 58 K. Finally, it is useful to point out an interesting fact about oxygen underdoping which has not been revealed by previous studies. As can be noted from the channeling portions of Fig. 1(c) (lower panel), the "channeled" oxygen contribution in the underdoped case is actually higher than that in the optimally doped sample. This implies that the process of introducing oxygen deficiency in the sample also causes lattice distortions leading to enhanced dechanneling in the measurement. These distortions may have a contribution to the suppression of the transition temperature in addition to the other factors.

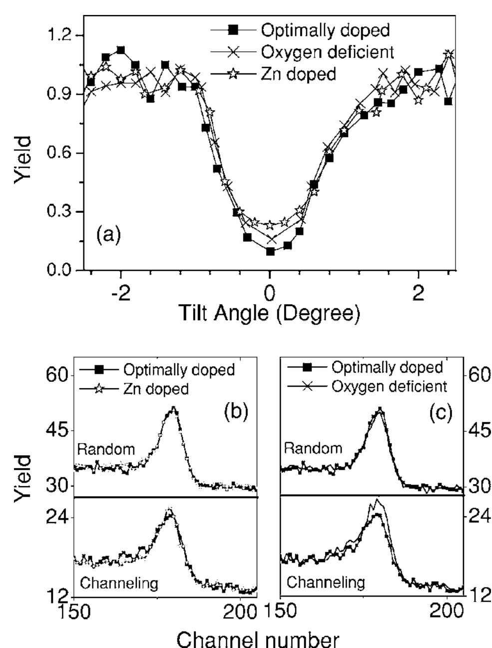

FIG. 1. Results of RBS, ion channeling, and oxygen determination studies: (a) The channeling angular scans for the optimally doped, underdoped, and Zn-doped samples grown on Nb:$SrTiO_3$; (b) comparison of oxygen yield in the resonance mode for the three cases in the normal and channeling modes.

The data for in-plane resistivity (ρ_{ab}) as function of temperature (T) for four samples (two optimally doped samples grown at 800 °C and 750 °C, Zn-doped and oxygen deficient samples) are shown in Fig. 2. It is evident that the transition temperature, T_O (onset), is 92 K, 58 K, and 45 K for the optimum-doped, oxygen-deficient and Zn-doped ($YBa_2Cu_{3-x}Zn_xO_{7-\delta}$, $x=0.2$) samples, respectively. The properties of the optimally doped sample are as expected in terms of the residual resistively ratio and the sharpness of

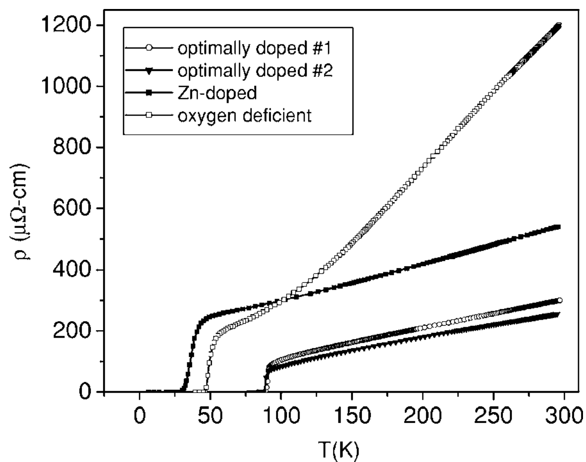

FIG. 2. The in-plane resistivity (ρ_{ab}) as a function of temperature (T) for the optimally doped (grown at 800 °C and 750 °C), underdoped, and Zn-doped films on $SrTiO_3$.

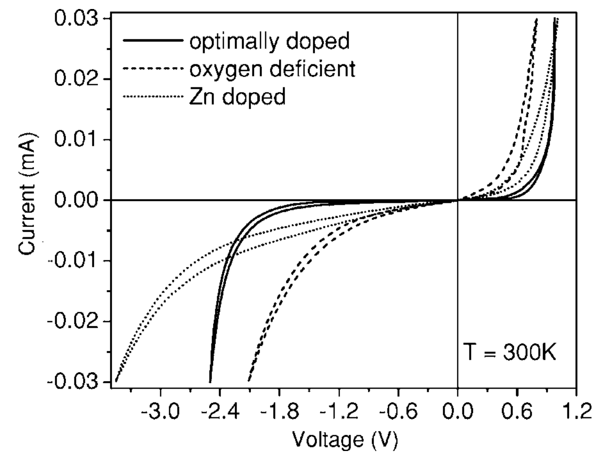

FIG. 3. Comparison of the room temperature I-V characteristics for the junctions based on optimally doped, oxygen deficient, and Zn-doped YBCO.

transition. The shift of the transition to lower temperature and its broadening as observed for the underdoped and Zn-doped samples are also consistent with the previous results.[48,51,52] The normal state resistivity values for the optimum-doped, oxygen-deficient and Zn-doped samples were found to be 300 ± 100 $\mu\Omega$ cm, 1200 ± 200 $\mu\Omega$ cm, and 540 ± 100 $\mu\Omega$ cm, respectively, and are in a reasonable agreement with the literature.

The primary effects of Zn doping[48] and related scattering is to add a nominally temperature independent contribution to the transport scattering rate. However, a small increase in the average slope of $d\rho_{ab}/dT$ can be noted and the same can be attributed either to a decrease in carrier concentration or some temperature dependent scattering contribution. Each Zn ion is suggested to represent a scattering cross section of a diameter of about 4.2 Å (encompassing four oxygen neighbors) and this strong scattering may well be one of the causes of the rapid suppression of T_c with Zn incorporation.[48] Zn is a nonmagnetic impurity, but it induces a magnetic moment in CuO_2 plane when substituted at the Cu site, the precise value of the moment being dependent upon oxygen content.

The peculiar S shape characteristic of the resistivity curve for the oxygen deficient film has been noted and discussed in the literature[52] for oxygen under-doped YBCO crystals, thin films, as well as for cobalt doped YBCO crystals, and is distinctly different as compared to a uniform upward shift in resistivity and decrease in the transition temperature seen for Zn doped films. Indeed the initial considerably higher slope ($d\rho/dT$) from 300 K down to about 125 K as compared to the case of optimally doped film, followed by the tapering off of the slope observed in our film is completely consistent with the reports in the literature.[52] The pronounced and systematic nonlinear behavior in oxygen deficient films has been attributed to reduced hole densities (electron doping) as analyzed by Hall measurements. The change in the slope of the T dependence of resistivity at an independent temperature corresponds to the change in the nature of dependence of Hall carrier density on temperature.

Figure 3 compares the room temperature I-V characteristics for the three cases of junctions based on optimally doped, oxygen deficient and Zn-doped YBCO. The general features in all the three cases appear to reflect the basic characteristics expected for a metal-semiconductor (M-S) junction, although there are clear differences between the optimally doped case and the two other cases of underdoped and Zn-doped films.

Figures 4(a), 4(c), and 4(e), show the current-voltage characteristics (I-V) for the three junctions (optimally doped, underdoped, and Zn-doped samples grown on Nb:STO) under forward biased conditions at some temperatures, with negative (positive) bias applied to NSTO (YBCO). The corresponding reverse biased characteristics are shown in Figs. 4(b), 4(d), and 4(f), respectively. No superconductivity related features (expected in the meV range) could be seen possibly due to the specific nature of interfacial layer formation and the role of the corresponding electronic states in suppressing the features. Also, hysteretic features are noted in the characteristics, which have been observed in previous works[61–64] on perovskite matrices and attributed to complex effects involving interface trap states, oxygen vacancy defects and their slow dynamics under current and field driven by electrochemistry.[65–68] Such effects can lead to distribution of charge in the interfacial region affecting the band line-up and tunneling probability. Clearly, the degree of hysteretic characteristic should differ in the three cases being discussed herein. In the underdoped and Zn-doped cases the leakage current density on reverse bias is also comparatively higher. For comparison, the room temperature values of reverse current density (J_{rev}) at -1 V bias for optimally doped, underdoped, and Zn-doped films are $\sim6\times10^{-4}$ A/cm^2, 18×10^{-4} A/cm^2, 27×10^{-3} A/cm^2, respectively. The relatively large values of reverse current densities are expected for the small barrier widths arising from a large carrier concentration in NSTO due to a high Nb concentration. With much lower Nb concentration such as 0.01 wt. % one should be able to reduce J_{rev} substantially. It may further be noted that for this oxygen deficient case, at intermediate and low temperatures one observes large excess current in the reverse region, exhibiting a more symmetrical behavior at small voltages. Similar symmetric nonlinearity was also seen in the

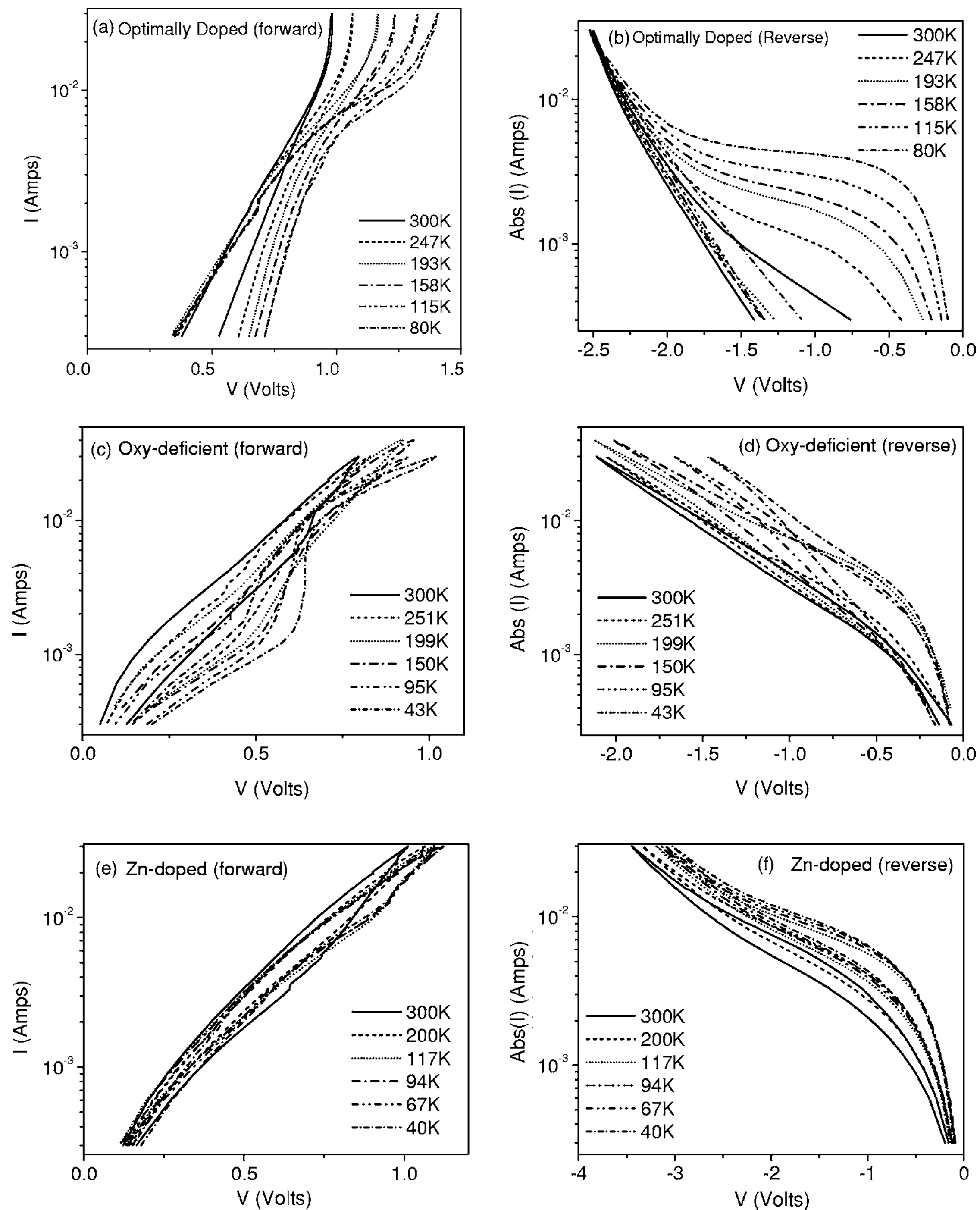

FIG. 4. Current-voltage (*I-V*) characteristics for YBCO/Nb:$SrTiO_3$ junctions: (a), (c), and (e) correspond to the forward bias (lower current curve in the hysteresis representing the positive going trace), and (b), (d), and (f) to reverse bias (higher current curve in the hysteresis representing the negative going trace), for junctions with optimally doped, Zn-doped, and oxygen underdoped YBCO films, respectively.

optimally doped case but at temperatures below about 60 K and in Zn-doped case even at relatively higher temperatures. The origin of this contribution is not clear at this time.

Before we proceed to discuss the observed transport data, it is important to mention that we ensured the high quality of our interfaces by high resolution scanning transmission electron microscopy (STEM); the representative data for an optically doped film being shown in Fig. 5. The interface is clearly seen to be abrupt and epitaxial. The stacking fault type features running parallel to the interface are well known in the highest quality films.[69] Scattered nanoscale inclusions which are also known in high quality films were noted, but their being mostly away from the interface should not influence the intrinsic features of the interface transport problem at hand. We have also performed chemical analysis of the films across the interface using electron loss spectroscopy

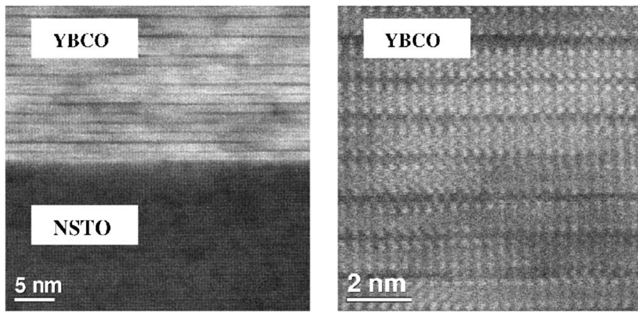

FIG. 5. High resolution scanning transmission electron microscopy (STEM) data for optimally doped YBCO films grown on Nb:$SrTiO_3$.

(EELS) and found that the interfaces are also chemicaly sharp within subnanometer scale. The details of these studies will be reported separately.[70] As discussed earlier, the high epitaxial quality of the films was separately established through RBS channeling results.

Over a decade ago, Hasegawa *et al.*[71] had studied the properties of the contact between the high-T_c superconductor Er-Ba-Cu-O and Nb:STO for two cases of Nb doping (0.05 wt. % and 0.5 wt. %) in STO. The T_c (zero resistance) of their optimally doped film was 69 K much lower than the expected 92 K.[72] It may be noted that the T_c in our optimally doped films was ~91 K. As in our case, these authors had also not observed any superconductivity related structure in the *I-V* characteristics, which is expected in the meV regime. As pointed out by Hasegawa *et al.* this nonobservance can be attributed to the presence of some interfacial layer or states on the surface of the semiconductor Nb:STO. These authors had found that with decreasing temperature the forward current decreases while the reverse current increases. In their sample with higher Nb content (0.5% resembling our case) they observed that both the forward and reverse currents were relatively higher as compared to those for lower Nb (0.05 wt. %) doped sample, and the *I-V* characteristic was less temperature dependent. The latter suggested that tunneling current is dominant in this case. Defining the reverse breakdown voltage as the voltage at which the reverse current density becomes 1×10^{-4} A/cm^2, these authors examined the temperature dependence of the breakdown voltage. In the sample with 0.5 wt. % (heavy) Nb doping, which is closer to our case, the breakdown voltage was lower as compared to the lower Nb doped (0.05 wt. %) sample, and it showed only weak temperature dependence. In the heavily Nb doped sample the Schottky barrier is thin causing tunneling current to increase. This in turn causes an increase in the Zener breakdown contribution, leading to a relatively lower breakdown voltage and its weak temperature dependence.

It is now useful to comment on the applicability of specific models for analyzing transport across a metal-semiconductor junction to the situation at hand, which represents the case of a heavily doped wide band-gap oxide semiconductor in contact with an oxide metal having high carrier concentration. The transport across a Schottky contact can be analyzed within the frameworks of the thermionic emission theory, diffusion theory or a hybrid theory accounting for both the effects, depending on the specifics of the problem, because of the different assumptions of the models.[20]

For the case moderately doped high mobility semiconductors the thermionic model is generally applicable. In this case the *I-V* relation for the current flow through a Schottky contact is given by

$$I = I_{sT}[\exp(qV/nkT) - 1], \tag{1}$$

where q is the electronic charge, k is the Boltzmann constant, V is the bias voltage and n is the ideality factor. The reverse saturation current I_{sT} is given by

$$I_{sT} = AA^{**}T^2 \exp(-q\varphi_B/kT), \tag{2}$$

where A is the diode area,A^{**} is the effective Richardson constant, and φ_B is the apparent barrier height.

For the diffusion theory, which is generally applicable for low mobility semiconductors, the current density expression is similar to the thermionic emission theory:

$$I = I_{sD}[\exp(qV/nkT) - 1]. \tag{3}$$

However, the saturation current density has a different form given by

$$I_{sD} = \frac{q^2 D_n N_C}{kT}\left[\frac{q(V_{bi} - V)2N_D}{\varepsilon_s}\right]^{1/2} \exp(-q\varphi_B/kT). \tag{4}$$

Here D_n is the diffusion coefficient, N_C is the effective density of states in the conduction band, V_{bi} is the built-in potential, V is the applied potential, ε_s is the semiconductor permittivity, and N_D is the donor impurity density. A few things can be noted from the comparison of Eqs. (2) and (4). First, I_{sD} varies more rapidly with the voltage but is less sensitive to the temperature as compared to I_{sT}. Second, I_{sD} depends on N_D, which is not the case for pure thermionic theory. Third, over low voltage range $(V \ll V_{bi})$ the extra voltage dependence of Eq. (4) will weaken yielding voltage dependence only from the exponential term in Eqs. (1) and (3).

Although $SrTiO_3$ has fairly high carrier mobility for an oxide, it is certainly not high enough to eliminate the possible contribution of diffusion model to our case. Moreover, we did observe that the *I-V* characteristics depend on Nb concentration (data not shown), further implying a role of carrier diffusion. It is also clear however that even within the framework of diffusion model a more realistic estimate of the effective Schottky barrier height should be possible by restricting to low voltage regime $(V \ll V_{bi})$. Finally, it is important to recognize that in our current case of fairly heavily doped semiconductor, the tunneling current also makes an important contribution. The modified equations then lead to the definition of ideality factor given by the relation

$$n = \frac{1}{2.3026 \times kT/q \times d(\log I)/dV}. \tag{5}$$

As Sze[20] has pointed out, the ideality factors can depart substantially from unity in the case of heavily doped semiconductors (as in our case), the departure increasing with lowering temperature.

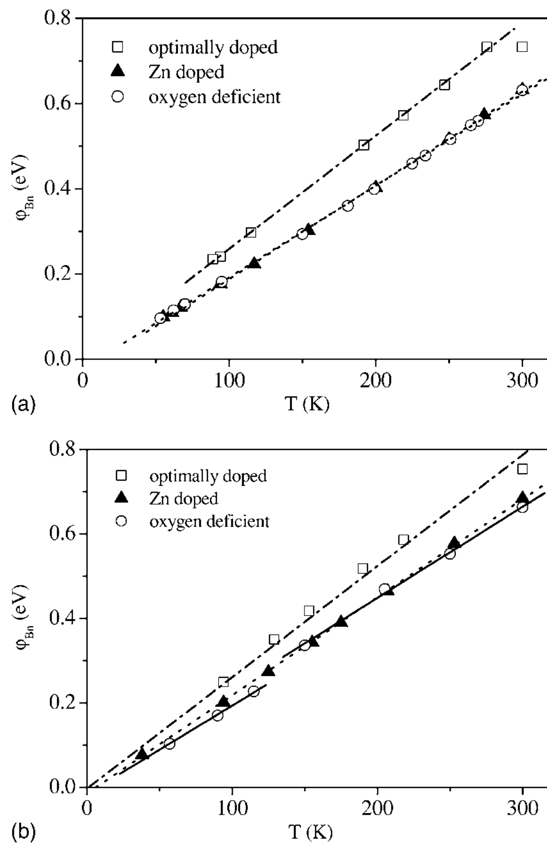

FIG. 6. Dependence of the effective Schottky barrier height (SBH) on temperature for optimally doped, underdoped, and Zn-doped films on $SrTiO_3$ obtained from Eq. (1) (a) over larger current range (5–20 mA), and (b) over low current regime (0–5 mA).

In Fig. 6(a) we show the dependence of the effective Schottky barrier height (SBH, denoted by Φ_B), calculated using the rising portions of the forward biased *I-V* curves. The observed decrease in SBH with temperature reflects the degree of non-ideality of the junctions which we address later. The rates of decrease of Φ_B with temperature for the optimally doped, Zn-doped and oxygen deficient cases are (a) optimally doped film: 2.6 meV/K, (b) Zn-doped film: 2.2 meV/K, and (c) oxygen deficient film: 2.15 meV/K. The room temperature values of the ideality factor n are (a) optimally doped film: 4.4, (b) Zn-doped film: 7.7, and (c) oxygen deficient film: 7.27. The significant departure of n from unity can be attributed to the heavily doped nature of the semiconductor.[20] Interestingly the values for the Zn-doped and oxygen deficient films are considerably higher than the optimally doped case. The rate of increase of n with decreasing temperature (not shown) is also much smaller in the optimally doped case as compared to the other two cases. The value of SBH (Φ_B) at room temperature is found to be $\sim 0.73 \pm 0.02$ eV for the case of the optimally doped YBCO films, $\sim 0.63 \pm 0.02$ eV for the Zn-doped and oxygen deficient cases. Here the indicated deviation around the mean value reflects the sample to sample variation. The smallness of this deviation reflects the robustness of the numbers, making them worthy of analyses. It also speaks for the intrinsic nature of the changes observed between different cases considered. It is interesting that the SBH values for the oxygen underdoped and Zn-doped YBCO films are lower than those for optimally doped YBCO cases but close to each other; the two cases representing considerably suppressed but closely placed superconducting transitions. We found that the SBH value for the optimally doped film grown at 750 °C is also close to 0.73 ± 0.02 eV, which establishes that the decrease in SBH for the junction based on Zn-doped film is not due to growth condition related change, but is intrinsic to Zn doping. Given the connection between the transition temperature and the density of states at the Fermi energy (ρ_{EF}), this result reflects the role of ρ_{EF} in defining Φ_B and possibly the related changes in the work function. Clearly, these differences are small because they should appear via shifts in the weight of a distribution. In Fig. 6(b) we show the SBH dependence on temperature for the three cases, estimated by restricting only to the low current regimes ($\leqslant 5$ mA) to see whether any unexpected contributions at higher current influence the calculated SBH values significantly. The changes are rather small, but we do see an interesting feature resolved in the oxygen deficient case, which relates to the corresponding *S*-shaped resistivity curve shown in Fig. 2. For this case we observe a distinct downward jump of about 40–50 meV near ~ 125 K, which also corresponds to the temperature at which the resistivity dependence on temperature (Fig. 2) shows a change in the slope. As pointed out earlier, over low voltage (and therefore current) range ($V \ll V_{bi}$) the extra voltage dependence of Eq. (4) corresponding to carrier diffusion effects is weak yielding a voltage dependence only from the exponential term in Eqs. (1) and (3). The SBH values obtained from the form of Eq. (1) employed over low voltage (current) range, presented in Fig. 6(b), may thus reveal the intrinsic features more clearly, such as the feature near 125 K for oxygen underdoped case. When the same equation is employed over a broader voltage range [as in Fig. 6(a)] some such fine features could be wiped out because of the partial inapplicability of Eq. (1).

As discussed by Singh *et al.*[37] the mechanisms contributing to the effective Schottky barrier height (SBH) and ideality factor n of metal-semiconductor (MS) junctions and their interplay leading to a specific nature of temperature (T) dependence of SBH and n have been the subjects of many interesting scientific investigations over the past few decades.[19–26] Many theoretical models developed and discussed in this respect hinge upon the notion of Fermi level (E_F) pinning by the electronic midgap states or the interface defect states the corresponding T dependence being suggestive of the mechanism of Fermi level pinning. For an E_F pinned by midgap states, the T dependence of the barrier height should mimic that of the band gap. However, if E_F is pinned by the interface defects, the T dependence of the SBH is controlled by the ionization entropy of such defects. The differences between the T dependences in the two cases should, in principle, allow one to discern the operative pinning mechanism in the specific case. Card and Rhoderick[19] have shown that the ideality factor for a Schottky diode is related to the density of interface states between the metal and semiconductor by the equation

$$n = 1 + \frac{(\delta/\varepsilon_i)(\varepsilon_s/W + qD_{sb})}{1 + (\delta/\varepsilon_i)qD_{sa}}.$$

Here δ is the thickness of the insulating surface layer, W is the width of the depletion region in the semiconductor, and ε_i and ε_s are the permittivities of the insulating layer and the semiconductor, respectively. Also, D_{sa} and D_{sb} represent the density of states that are in equilibrium with the metal and the semiconductor, respectively. Clearly, a higher density of the interface states in equilibrium with the semiconductor as controlled by the corresponding Fermi energy (D_{sb}) increase the ideality factor n. As Dharmadasa *et al.*[22] have discussed, the value of D_{sb} and the energy positions of the corresponding states in the band have implications for the value of SBH as well as the precise nature of the *I-V* characteristics. However, in all these theoretical models a laterally homogeneous SBH is presumed and the role of SBH inhomogeneity, which can occur under most realistic experimental conditions, is not addressed. Indeed, experimental investigations have established the existence of such nanoscale local non-uniformities of SBH. Tung has modeled and analyzed the implications of such SBH inhomogeneity for the properties such as the integral SBH.[8,23] Assuming nanoscale lateral variations in local SBH he has been able to offer satisfactory explanation of the temperature evolution of the apparent barrier height (Φ_B) and ideality factor (n). It is very important to mention here that the effects discussed by Tung occur when the length scale of lateral fluctuations is smaller than the width of the depletion layer width W. On the other hand, if the fluctuations are on a longer length scale than W, regions with different local SBHs are essentially electrically independent and the total junction current is a sum of currents through different areas.[73]

In our case, the observed, rather strong temperature dependence of SBH ($\sim 2.2\pm 0.1$ meV/K) cannot be explained by midgap or interface state pinning mechanisms. This is because the value of temperature coefficient of SBH for the case of midgap state pinning, which mimics the band-gap change, cannot be stronger than a very small fraction of the above values. Also, the ionization entropy of the interface defects depends only very weakly on temperature.[37] Thus, as in the case of many real Schottky junctions, in our case the lateral nanoscale SBH inhomogeneity as proposed and analyzed by Tung[23] and Werner and Guttler[24] appear to be responsible for the observed dependences of Φ_B and n on T. Assuming a Gaussian type distribution function for SBH inhomogeneity, Dobrocka and Osvald[26] have shown that this dependence is strongest for the largest standard deviation of the distribution function.

In real junctions lateral inhomogeneity could result from factors such as strain, chemical composition or interface topological fluctuations, defect distributions etc. There can also be intrinsic electronic inhomogeneity in the two layers forming the junction which would manifest in the *I-V* response. The fact that the temperature variation of Φ_B correlates with the *S*-shaped resistivity dependence on temperature in the case of the junction based on oxygen deficient film is important to note in this context. Also, a higher degree of nonideality in oxygen deficient and Zn-doped case could possibly be due to the sensitivity of local electronic states to Zn or oxygen vacancy concentration and the natural lateral fluctuations in these. One may also need to consider the fluctuations in the concentration of Niobium in the substrate (NSTO) which would cause changes in the local carrier concentration and thereby fluctuations in SBH. Given the use of heavily doped (0.5 wt. %) Nb:$SrTiO_3$ semiconductor in our experiments implying small depletion width W, our observations suggest that nanoscale electrical property fluctuations are present in the optimally doped, underdoped and Zn-doped YBCO film even in the normal state. Presence of nanoscale electrical property fluctuations in oxide superconductors have indeed been addressed in the literature.[54–56,58,59,74] Pan *et al.* have shown that such inhomogeneity manifests in the form of spatial variations in both the local density of states spectrum and the superconducting energy gap. These occur over surprisingly short length scale of the order of 1–2 nm. Lang *et al.* have shown an apparent segregation of the electronic structure into domains of ~ 3 nm reflecting the hole redistribution. Since SBH is basically the difference between the metal work function and the electron affinity of the semiconductor,[20] the basic manifestation of the inhomogeneity in the effective SBH must emanate from the inhomogeneity in the superconductor work function. Indeed such nanoscale work function inhomogeneity has been reported in oxide superconductors by direct STM studies.[75,54–56] In the case of superconductors (optimally doped, oxygen underdoped, and Zn-doped) there could be a close connection of the work function fluctuations to the modulations of carrier density.

It is interesting to point out here that inhomogeneity over different length scales has been reported in different mixed-valent colossal magnetoresistance manganite systems.[76] Yet, in specific cases involving manganite electrode ($La_{0.67}Sr_{0.33}MnO_3$) in contact with Nb:$SrTiO_3$ nearly ideal Schottky characteristics have been recently realized.[77] The reason for this can be attributed to (a) much larger length scale of electronic phase separation (and the corresponding electrical property fluctuation) in the more metallic LSMO system (as compared to cases such as ($La_{0.67}Ca_{0.33}MnO_3$ or $Pr_xLa_{0.67-x}Ca_{0.33}MnO_3$),[76] (b) major differences in the electrical properties of the two components in the phase separated state (ferromagnetic metal and charge ordered insulator),[76] and (c) use of 0.01 wt. % and 0.1 wt. % Nb:$SrTiO_3$ substrates yielding larger value of depletion width W, reducing tunneling contribution (as against the case of 0.5 wt. % Nb:$SrTiO_3$ in the present work).

IV. CONCLUSIONS

The properties of Schottky junctions formed by pulsed laser deposited films of optimally doped, underdoped, and Zn-doped $YBa_2Cu_3O_{7-\delta}$ on single crystal (001) 0.5 wt.% Nb:$SrTiO_3$ substrates were examined. The growth conditions were optimized in each case to get the appropriate crystalline quality of the films as well as the desired normal state and superconducting properties. The high quality of the films as well as the interfaces was established using different appropriate techniques. Nonlinear *I-V* curves (forward and reverse) were obtained in all cases. Analyses of these data brought out the intrinsic differences between the parametric values in the three cases, as well as the temperature variation of the Schottky Barrier Height (SBH, Φ) and the ideality

factor (n) in each case. The small but definitive lowering of Φ in the case of oxygen underdoped and Zn-doped YBCO reflects the role of ρ_{EF} in defining Φ_B and possibly the related changes in the work function. These differences are small because they should appear via shifts in the weight of a distribution. The systematics of temperature dependence of Φ and n can be accounted for within the model of nanoscale electrical property inhomogeneity. Given the high quality of interfaces, we suggest that this inhomogeneity is intrinsic in nature. Interesting correlation is noted between the S-shaped resistivity dependence on T in the oxygen deficient sample and the temperature variation of SBH estimated over low current regime, bringing out an energy shift of about 40 meV at the inflection point.

ACKNOWLEDGMENTS

One of the authors (W.R.) will like to thank the Fulbright commission for support. The authors would like to thank Richard Greene for fruitful discussions. The work was performed using the shared experimental facilities (SEFs) of pulsed laser deposition and Pelletron accelerator supported by the Center for Superconductivity Research and UMD NSF-MRSEC Grant No. DMR 00-80008. The microscopy work (N.D.B.) was supported by NSF Grant No. DMR-0335364 and performed in the National Center for Electron Microscopy at Lawrence Berkeley National Laboratory supported by the Department of Energy under Contract No. DE-AC03-73SF00098.

[1] T. Ando, A. B. Fowler, and F. Stern, Rev. Mod. Phys. **54**, 437 (1982).
[2] V. A. Markov and S. Stoyanov, Contemp. Phys. **28**, 267 (1987).
[3] P. Batra, E. Tekman, and S. Ciraci, Prog. Surf. Sci. **36**, 289 (1991).
[4] G. P. Das, Pramana, J. Phys. **38**, 545 (1992).
[5] A. Franciosi and C. G. VandeWalle, Surf. Sci. Rep. **25**, 1 (1996).
[6] M. Peressi, N. Binggeli, and A. Baldereschi, J. Phys. D **31**, 1273 (1998).
[7] G. Margaritondo, Rep. Prog. Phys. **62**, 765 (1999).
[8] R. T. Tung, Mater. Sci. Eng., R. **35**, 1 (2001).
[9] S. P. Wilks, J. Phys. D **35**, R77 (2002).
[10] B. T. Jonker, Proc. IEEE **91**, 727 (2003).
[11] J. M. Triscone and O. Fischer, Rep. Prog. Phys. **60**, 1673 (1997).
[12] D. P. Norton, Annu. Rev. Mater. Sci. **28**, 299 (1998).
[13] K. Ueda, H. Tabata, and T. Kawai, Science **280**, 1064 (1998).
[14] G. D. Wilk, R. M. Wallace, and J. M. Anthony, J. Appl. Phys. **89**, 5243 (2001).
[15] A. Ohtomo, D. A. Muller, J. L. Grazul, and H. Y. Hwang, Nature (London) **419**, 378 (2002).
[16] A. Ohmoto and H. Y. Hwang, Nature (London) **427**, 423 (2004).
[17] Y. Ijiri, J. Phys.: Condens. Matter **14**, R947 (2002).
[18] D. P. Norton, Mater. Sci. Eng., R. **43**, 139 (2004).
[19] H. C. Card and E. H. Rhodreick, J. Phys. D **4**, 1589 (1971).
[20] S. M. Sze, *Physics of Semiconductor Devices*, 2nd ed. (Wiley Interscience, New York, 1981).
[21] J. L. Freeouf, T. N. Jackson, S. E. Laux, and J. M. Woodall, Appl. Phys. Lett. **40**, 634 (1982).
[22] I. M. Dharmadasa, G. G. Roberts, and M. C. Petty, J. Phys. D **15**, 901 (1982).
[23] R. T. Tung, Appl. Phys. Lett. **58**, 2821 (1991).
[24] J. H. Werner and H. H. Guttler, Appl. Phys. Lett. **56**, 1113 (1990); J. Appl. Phys. **69**, 1522 (1991); J. Appl. Phys. **73**, 1315 (1993).
[25] J. P. Sullivan, R. T. Tung, and M. R. Pinto, J. Appl. Phys. **70**, 7403 (1991).
[26] E. Dobrocka and J. Osvald, Appl. Phys. Lett. **65**, 575 (1994).
[27] V. G. Bozhkov and D. Ju. Kuzyakov, J. Appl. Phys. **92**, 4502 (2002).
[28] L. L. Chang and C. M. Hu, Superlattices Microstruct. **28**, 351 (2000).
[29] H. Morkoc and Y. Taur, J. Korean Phys. Soc. **42**, S 555 (2003).
[30] S. E. Thompson, R. S. Chou, T. Ghani, K. Mistry, S. Tyagi, and M. T. Bohr, IEEE Trans. Semicond. Manuf. **18**, 26 (2005).
[31] S. B. Ogale, V. Talyansky, C. H. Chen, R. Ramesh, R. L. Greene, and T. Venkatesan, Phys. Rev. Lett. **77**, 1159 (1996).
[32] D. M. News, J. M. Misewich, C. C. Tsuei, A. Gupta, B. A. Scott, and A. Schrott, Appl. Phys. Lett. **73**, 780 (1998).
[33] T. Venkatesan, M. Rajeswari, Z. W. Dong, S. B. Ogale, and R. Ramesh, Philos. Trans. R. Soc. London, Ser. A **356**, 1661 (1998).
[34] Y. Tokura and Y. Tomioka, J. Magn. Magn. Mater. **200**, 1 (1999).
[35] T. Wu, S. B. Ogale, J. E. Garrison, B. Nagaraj, A. Biswas, Z. Chen, R. L. Greene, R. Ramesh, T. Venkatesan, and A. J. Millis, Phys. Rev. Lett. **86**, 5998 (2001).
[36] T. Minami, MRS Bull. **25**, 38 (2000).
[37] R. Singh, S. K. Arora, R. Tyagi, S. K. Agarwal, and D. Kanjilal, Bull. Mater. Sci. **23**, 471 (2000).
[38] H. Tanaka, J. Zhang, and T. Kawai, Phys. Rev. Lett. **88**, 027204 (2002).
[39] F. X. Hu, J. Gao, J. R. Sun, and B. G. Shen, Appl. Phys. Lett. **83**, 1869 (2003).
[40] A. Tiwari, C. Jin, D. Kumar, and J. Narayan, Appl. Phys. Lett. **83**, 1773 (2003).
[41] J. R. Sun, C. M. Xiong, T. Y. Zhao, S. Y. Zhang, Y. F. Chen, and B. G. Shen, Appl. Phys. Lett. **84**, 1528 (2004).
[42] J. R. Sun, C. M. Xiong, B. G. Shen, P. Y. Wang, and Y. X. Weng, Appl. Phys. Lett. **84**, 2611 (2004).
[43] J. R. Sun, C. M. Xiong, Y. F. Chen, B. G. Shen, and L. Kang, Europhys. Lett. **66**, 868 (2004).
[44] J. R. Sun, C. H. Lai, and H. K. Wong, Appl. Phys. Lett. **85**, 73 (2004).
[45] T. Muramatsu, Y. Muraoka, and Z. Hiroi, Solid State Commun. **132**, 351 (2004).
[46] M. Ziese, U. Kohler, R. Hohne, A. Bollero, and P. Esquinazi, J. Magn. Magn. Mater. **290**, 1116 (2005).
[47] C. Ren, J. Trbovic, P. Xiong, and S. Von Molnar, Appl. Phys. Lett. **86**, 012501 (2005).
[48] T. R. Chien, Z. Z. Wang, and N. P. Ong, Phys. Rev. Lett. **67**, 2088 (1991).
[49] J. M. Harris, Y. F. Yan, and N. P. Ong, Phys. Rev. B **46**, R14293 (1992).

[50] T. Ito, K. Takenaka, and S. Uchida, Phys. Rev. Lett. **70**, 3995 (1993).
[51] Y. Fukuzumi, K. Mizuhashi, K. Takenaka, and S. Uchida, Phys. Rev. Lett. **76**, 684 (1996).
[52] B. Wuyts, V. V. Moshchalkov, and Y. Bruynseraede, Phys. Rev. B **53**, 9418 (1996) and references therein.
[53] R. P. Sharma, S. B. Ogale, Z. H. Zhang, J. R. Liu, W. K. Chu, B. Veal, A. Paulikas, H. Zheng, and T. Venkatesan, Nature (London) **404**, 737 (2000).
[54] S. H. Pan, J. P. O'Neal, R. L. Badzey, C. Chamon, H. Ding, J. R. Engelbrecht, Z. Wang, H. Eisaki, S. Uchida, A. K. Gupta, K.-W. Ng, E. W. Hudson, K. M. Lang, and J. C. Davis, Nature (London) **413**, 282 (2001).
[55] D. N. Shi, Z. D. Wang, and J. X. Li, Physica C **371**, 69 (2002).
[56] K. M. Lang, V. Madhavan, J. E. Hoffman, E. W. Hudson, H. Eisaki, S. Uchida, and J. C. Davis, Nature (London) **415**, 412 (2002).
[57] Z. Y. Chen, A. Biswas, I. Zutic, T. Wu, S. B. Ogale, R. L. Greene, and T. Venkatesan, Phys. Rev. B **63**, 212508 (2001).
[58] E. Li, R. P. Sharma, S. B. Ogale, Y. G. Zhao, T. Venkatesan, J. J. Li, W. L. Cao, and C. H. Lee, Phys. Rev. B **65**, 184519 (2002).
[59] E. Li, S. B. Ogale, R. P. Sharma, T. Venkatesan, J. J. Li, W. L. Cao, and C. H. Lee, Phys. Rev. B **69**, 134520 (2004).
[60] S. B. Ogale, M. Rajeswari, R. P. Sharma, and T. Venkatesan, Appl. Phys. Lett. **68**, 421 (1996).
[61] A. Yoshida, H. Tamura, K. Gotoh, H. Takauchi, and S. Hasuo, J. Appl. Phys. **70**, 4976 (1991).
[62] A. Baikalov, Y. Wang, B. Shen, B. Lorenz, S. Tsui, Y. Y. Sun, Y. Y. Xue, and C. W. Chu, Appl. Phys. Lett. **83**, 957 (2003).
[63] A. Sawa, T. Fujii, M. Kawasaki, and Y. Tokura, Appl. Phys. Lett. **85**, 4073 (2004).
[64] T. Fujii, M. Kawasaki, A. Sawa, H. Akoh, Y. Kawazoe, and Y. Tokura, Appl. Phys. Lett. **86**, 012107 (2005).
[65] B. W. Veal, H. You, A. P. Paulikas, H. Shi, Y. Fang, and J. W. Downey, Phys. Rev. B **42**, 4770 (1990).
[66] B. H. Moeckly, D. K. Lathrop, and R. A. Buhrman, Phys. Rev. B **47**, 400 (1993).
[67] N. Chandrasekhar, O. T. Valls, and A. M. Goldman, Phys. Rev. Lett. **71**, 1079 (1993).
[68] S. H. Huerth, M. P. Taylor, H. D. Hallen, and B. H. Moeckly, Appl. Phys. Lett. **77**, 2127 (2000).
[69] R. Ramesh, D. M. Hwang, T. Venkatesan, T. S. Ravi, L. Nazar, A. Inam, X. D. Wu, B. Dutta, G. Thomas, A. F. Marshall, and T. H. Gaballe, Science **247**, 57 (1990).
[70] L. F. Fu *et al.* (unpublished).
[71] H. Hasegawa, T. Fukazawa, and T. Aida, Jpn. J. Appl. Phys., Part 2 **28**, L2210 (1989).
[72] J. H. Takemoto, C. M. Jackson, H. M. Manasevit, D. C. St. John, J. F. Burch, K. P. Daly, and R. W. Simon, Appl. Phys. Lett. **58**, 1109 (1991).
[73] I. Ohdomari and K. N. Tu, J. Appl. Phys. **51**, 3735 (1980).
[74] H. A. Mook, P. C. Dai, F. Dogan, and R. D. Hunt, Nature (London) **404**, 729 (2000).
[75] J. F. Jia, Y. Hasegawa, T. Sakurai, and H. Zhang, Solid State Commun. **105**, 533 (1998).
[76] *Colossal Magnetoresistive Oxides*, edited by Y. Tokura (Gordon and Breach, New York, 2000); M. Uehara, S. Mori, C. H. Chen, and S.-W. Cheong, Nature (London) **399**, 560 (1999); J. Burgy, A. Moreo, and E. Dagotto, Phys. Rev. Lett. **92** 097202 (2004), and references therein.
[77] F. M. Postma, R. Ramaneti, T. Banerjee, H. Gokcan, D. H. A. Blank, R. Jansen, and J. C. Lodder, J. Appl. Phys. **95**, 7324 (2004).